This is an open access article published under an ACS AuthorChoice License, which permits copying and redistribution of the article or any adaptations for non-commercial purposes.

THE JOURNAL OF PHYSICAL CHEMISTRY C

Article

Cite This: J. Phys. Chem. C 2017, 121, 27643−27654

pubs.acs.org/JPCC

Silver Nanoparticles Synthesized by Microwave Heating: A Kinetic and Mechanistic Re-Analysis and Re-Interpretation

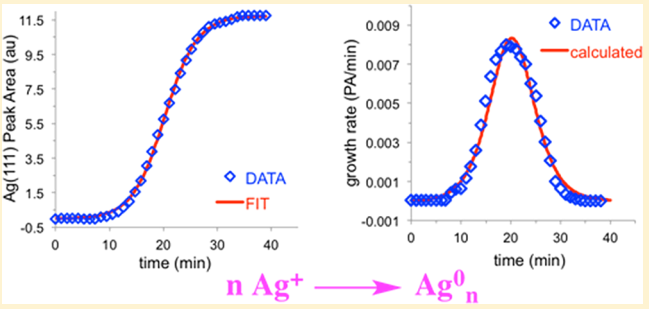
Saim Özkar[†,§] and Richard G. Finke*[,‡]

[†]Department of Chemistry, Middle East Technical University, 06800 Ankara, Turkey

[‡]Department of Chemistry, Colorado State University, Fort Collins, Colorado 80523, United States

Supporting Information

ABSTRACT: A quantitative kinetics and mechanistic re-analysis is performed of an important 2016 paper that described the formation of Ag_n nanoparticles from the polyol reduction of silver nitrate in the presence of poly(*N*-vinylpyrrolidone) under microwave heating. Elegantly and expertly obtained, in operando synchrotron high-energy X-ray diffraction (HEXRD) data, integrated with the microwave heating for the first time, were used to follow the Ag_n nanoparticle formation reaction in real time and to obtain time-resolved, HEXRD peak areas for the formation of both Ag(111) and Ag(200) facets. Unfortunately, the subsequent kinetics and mechanistic analysis that resulted is far from the state-of-the-art and was done without citing nor using well-established literature of nanoparticle nucleation and growth kinetics and mechanisms that has been available for over 20 years. Herein, the data are re-analyzed and re-interpreted in light of the fitting of the kinetics data with the presently most widely cited and employed, deliberately minimalistic, disproof-based nanoparticle nucleation and growth mechanism, dating back to 1997, of the pseudoelementary steps of slow continuous nucleation, A → B (rate constant k_1), and then fast, autocatalytic surface growth, A + B → 2B (rate constant k_2), where A is the starting Ag^+ and B is the Ag^0 product. The two pseudoelementary step mechanism is shown to be able to account for the previously reported kinetics data even for these large, up to ∼100 nm (i.e., 0.1 μm) Ag_n nanoparticles, a remarkable result in its own right given that there are on the order of $\sim 10^7$ Ag(0) atoms in a ∼100 nm particle formed from the reduction of $\sim 10^7$ Ag^+ atoms in what must be $>10^7$ actual elementary steps. However, the k_2 rate constant in particular likely loses much of its value since it is an average over a large change in the percentage of surface atoms in the growing nanoparticle. The results lead to nine revisions of questionable to incorrect previous claims and conclusions, plus a series of eight insights and guidelines for future work in nanoparticle formation kinetics and mechanism. An extensive Supporting Information further discusses interesting questions regarding the issues in analyzing and understanding nanoparticle formation kinetics and the mechanism of such large, ∼0.1 μm-sized particles.



INTRODUCTION

A 2016 paper[1] described the synthesis of Ag_n nanoparticles from the polyol reduction of silver nitrate in the presence of poly(*N*-vinylpyrrolidone) (PVP) under conditions of microwave heating. The TEM, HEXRD, UV−visible absorption spectroscopy, and other evidence provided[1] were sufficient to demonstrate that Ag^0_n nanoparticles are formed, initially of an average size of ∼9.9 nm as the first-observable particles (at t = 11 min; that were termed "seeds"[1]) and then growing to a broad distribution of average size ∼15 nm, then 104 nm, particles post >35 min at 140 °C. Elegantly obtained kinetics data in the 2016 paper resolved the formation of Ag(111) and Ag(200) facets for the first time. Additionally, others[2] have reported the microwave-assisted synthesis of Ag^0_n nanoparticles with a narrower size dispersion of 9.8 ± 0.9 nm achieved by a similar microwave-assisted polyol reduction of silver nitrate in the presence of PVP, and in a continuous flow reactor with a residence time of 2.8 s at 160 °C.[2] Hence, the microwave-assisted synthesis of Ag^0_n nanoparticles is of synthetic as well as kinetic and mechanistic interest.

Importance of the 2016 Paper. The aforementioned paper[1] employed powerful physical methods which yielded important, novel resultant kinetics data, notably: (i) the use of in operando synchrotron high-energy X-ray diffraction (HEXRD) integrated with microwave heating for the first time; (ii) the time-resolved, HEXRD-obtained peak areas of the Ag(111) and Ag(200) facets and, hence, novel quantitative kinetics data for the Ag(111) and Ag(200) peak areas vs time; hence, (iii) the ratio of Ag(111)/Ag(200) peak areas vs time; (iv) the Ag(111) linear dimension (in nm) vs time; and (v) the temperature dependence of the Ag(111) peak area vs time and, hence, the possibility of obtaining activation parameters for the formation of the Ag(111) facet for the first time. The expertly

Received: June 28, 2017
Revised: November 7, 2017
Published: December 1, 2017

Downloaded via ORTA DOGU TEKNIK UNIV on July 24, 2020 at 13:52:55 (UTC).
See https://pubs.acs.org/sharingguidelines for options on how to legitimately share published articles.

obtained, highly valuable experimental results—that were also demonstrated to be reproducible by the authors (e.g., see Figure S11 therein[1])—are noteworthy. That data provides a superior platform for addressing the kinetics and underlying mechanism of the Ag^0_n nanoparticle formation and their underlying nucleation, growth, and agglomeration, especially of the resolved Ag(111) and Ag(200) facets, in a way that was not previously possible.

Kinetics and Mechanistic Analysis in the 2016 Paper. Unfortunately, the kinetics and mechanistic analysis in the 2016 paper is not state-of-the-art. Specifically, (i) the analysis and interpretation of the kinetics and proposed mechanisms were done with a lack of citation of any of the following, well-established literature on the mechanisms of nanoparticle formation,[3−7] including key prior work on the mechanisms of Ag^0_n nanoparticle formation.[8−11] Additional issues with kinetics and mechanistic analysis provided[1] include that (ii) the kinetics of the full curves were not fit, see, for example, Figure 2A,C of the 2016 paper reproduced as Figure 1 herein. Instead, the first 10 min of the kinetics data are ignored, in part because a temperature heating ramp is being applied during the first ∼5−6 min of those 10 min. However, the problem in ignoring the full first 10 min of the kinetics data is that the crucial nucleation process is occurring during that key, early period.[12,13]

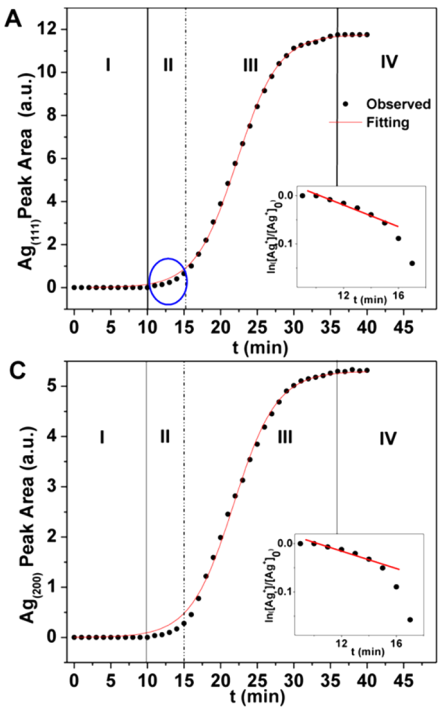


Figure 1. Reproduction of Figure 2A,C of the 2016 paper:[1] Variation of peak area of (A) Ag(111) and (C) Ag(200) reflections in the course of the $Ag^+ \rightarrow Ag^0$ reaction at 140 °C. The peak area was given in area units abbreviated as a.u. in the 2016 paper;[1] herein, the abbreviation au will be used instead in order to avoid confusion with atomic units (a.u.). The red curves represent the best fitting by the prior authors while employing an arbitrary, empirical sigmoidal function, as discussed more in the main text. Note that use of that empirical sigmoidal function provides a poor fit (red line) to the ∼8−17 min induction period part of the kinetics data. Insets present the linear fitting of $\ln([Ag^+]/[Ag^+]_0)$ as a function of reaction time at the early stage when crystalline Ag started to form. $[Ag^+]_0$ and $[Ag^+]$ represent the concentration of Ag^+ in the reaction solution before and after the reaction started, respectively. Note also that the claimed linear fits in the inset are over a very limited, arbitrary part of the kinetics data and are not really linear in any event. Reproduced with permission from the 2016 paper.[1] Copyright 2016 American Chemical Society.

A third issue is that (iii) the next ∼10−15 min of kinetics data were taken and plotted using an assumed rate law $\propto[Ag^+]^1[HOCH_2CH_2OH]^1$, that is, a rate law assumed to be first-order in $[Ag^+]$, despite growing precedent for a second-order rate law in the nucleating metal[8,14] (i.e., $\propto[Ag^+]^2$) having precedent and, hence, arguably being more probable.[8,14] Moreover, (iv) the initial natural log plots used to infer a first-order, $[Ag^+]^1$ dependence are nonlinear if examined carefully (see Figure 1 herein where those plots are reproduced, specifically the inset in Figure 1, vide infra) and, troublingly, the data used for those (poorly linear) log plots were taken over an arbitrary, limited part of the kinetics curve. One, of course, cannot "cherry pick" kinetics data out of just one part of a full kinetics curve, plot it this way as was done, and then assign any kind of reliable mechanistic meaning to it. Doing so is, instead, a recipe for being mislead kinetically and, hence, mechanistically.

Additional issues with the kinetics and mechanistic analysis of the data in the 2016 paper[1] are (v) that instead of using an established nanoparticle formation mechanism for fitting sigmoidal nanoparticle formation kinetics curves, for example, the widely employed FW two-step mechanism of slow continuous nucleation and then autocatalytic surface growth,[15] a mechanistically and physically meaningless empirical sigmoidal function of unreferenced origin was used, specifically, the function $Y = A_2 + (A_1 - A_2)/(1+ e^{(x-x_o)/dx})$ where Y stands for the peak area of Ag(111) or Ag(200) reflections, and x stands for time. Note also that this empirical function has three variables, A_1, A_2, and dx, whereas the FW two-step mechanism for example has just two variables, rate constants k_1 and k_2. In addition, the use of an empirical sigmoidal function as done previously[1] cannot, in turn, yield the desired rate constants—because rate constants can only come from, as they are defined only by, balanced chemical reactions.[16] Instead, mechanistically and physically useless—actually, worse, as we will see misleading (vide infra)—(empirical) rate parameters result from such empirical function fits,[6,7] all literally without any physically connected or meaningful concepts and words with which to describe the results. Hence, no physical or mechanistic insight is possible from such an empirical function fit, regardless of how hard one tries to generate such crucial, needed, bottom-line insights. (vi) Perhaps most importantly then—something that is crucial to correct as done herein—is that the putative mechanistic concepts and terms then used to (try to) describe the chemistry are, as a result of the use of empirical fitting functions, unconnected to any kinetics and mechanistic scheme and its corresponding differential equations. This is the insidious problem that continues to confound physical and mechanistic understanding when empirical functions are used to fit kinetics data, as we have demonstrated and discussed elsewhere,[6,7] and as is demonstrated herein. Finally, (vii) the lack of tracking of (i.e., lack of knowledge of) the Ag^+ to Ag^0 mass balance is another issue with the prior work.[1] Ideally, at least one complementary method to track the reaction would have been used (e.g., UV−vis or perhaps XANES) so that one could correlate the powerful HEXRD-based data to the absolute (vs just the relative) Ag^+ to Ag^0 mass changes in the reaction. The concentration of Ag^+ in the reaction solution at different times (at least in early stage) was calculated by subtracting the concentration of reduced Ag^+ from the initial

DOI: 10.1021/acs.jpcc.7b06323
J. Phys. Chem. C 2017, 121, 27643−27654

concentration, but it was not stated how the concentration of reduced Ag^+ was calculated nor was the conversion factor or calibration curve given to allow the needed quantitative connection between the HEXRD data and the $[Ag^+]$, nor is it apparent that an accounting for the minor, Ag(220) product and its HEXRD peak area is included as it should have been in the Ag^+ conversion calculations.

Focus of the Present Contribution. The present contribution aims to reanalyze and sort out conceptually the interesting results first reported in the 2016 paper.[1] Focal points include performing the kinetics and mechanistic analysis in light of what is known in the relevant literature on nanoparticle nucleation and growth, identifying recommended practices in such analyses (vs those that should be avoided), understanding better the issues in applying the deliberately minimalistic FW two-step mechanism to such large, ∼100 nm nanoparticle formation reactions, and construction of a list of remaining questions and, hence, needed additional experiments.

EXPERIMENTAL SECTION

System and Data. The senior author of the prior work[1] was contacted to see if he was willing to work together to yield a collaborative version of the present paper. Unfortunately, he declined our invitation, although he did share his questions, comments, and concerns on the penultimate version of the submitted manuscript, providing a number of thoughtful points that are acknowledged and addressed in the manuscript or Supporting Information (SI). Hence, we proceeded by digitizing the scanned plots of functional data by using the Java program Plot Digitizer Version 2.6.8. The synthesis of PVP-stabilized silver(0) nanoparticles and the system used for their in situ kinetics measurement and characterization are described in the 2016 paper.[1] However, there exist some subtleties that need to be noted here, namely: (i) it is 5−6 min before the microwave heating of the reaction solution from room temperature to 140 °C is fully complete (see the green arrows in Figure 1B in the 2016 paper[1]), so that the heating stage is convoluted at least somewhat with the nucleation stage of the kinetics. However, and fortunately, (ii) Figure 3B elsewhere[1] shows a strong temperature dependence in the observed kinetics so that relatively little nucleation is probably occurring until the temperature is close to ∼140 °C. Consistent with this, herein we find that if one drops just the first 3 min (the main heating stage) from the kinetics data obtained at 140 °C, then the best fit results to the FW two-step mechanism,[15,17,18] Figure 2 (vide infra) and Figure S1 of the SI. Another crucial aspect of the 2016 paper[1] is that it states, on page 716, that "Because the peak area in HEXRD-pattern is proportional to the mass of the corresponding crystalline materials with a pure crystalline phase, the variation of peak area as a function of reaction time can be used to track the reaction kinetics of nucleation and growth involved in the microwave reaction." Although unreferenced in the prior work,[1] this claim is supported by the XRD literature.[19−21] Accordingly, the peak area kinetics data[1] were used directly in this work as well for the kinetics and mechanistic re-analysis reported herein.

Note that even if one wanted to treat the kinetics data as the formation of a crystalline Ag^0 and, hence by, say, the semiempirical Avrami equation, the use of the FW two-step mechanism is still applicable since it has been shown to be the minimal chemical mechanism underlying the Avrami equation.[22] Moreover, using the chemical FW two-step mechanism avoids the problem, when using the Avrami equation, of having to try to interpret the problematic, nonphysical semiempirical "k" (rate parameter; *not* a rate constant) and "Avrami exponent", n, as discussed elsewhere.[22]

Kinetics Data Curve Fitting. The FW two-step mechanism consisting of slow, continuous nucleation (rate constant k_1) and autocatalytic surface growth (rate constant k_2) is given in eq 1.[15,17]

$$\begin{aligned} &A \xrightarrow{k_1} B \\ &A + B \xrightarrow{k_2} 2B \\ &\text{net } A \rightarrow B \end{aligned} \tag{1}$$

where, for the present system and analysis, A stands for the precursor Ag^+ ion and B for the growing A^0_n nanoparticles. The differential and integrated forms of its rate law[15] are given in eqs 2 and 3, respectively, all derived and discussed in detail in an earlier publication.[23]

$$-\frac{d[A]}{dt} = \frac{d[B]}{dt} = k_{1obs}[A]_t + k_{2obs}[A]_t[B]_t \tag{2}$$

$$[B]_t = [A]_0\left(1 - \frac{k_1 + k_2[A]_0}{k_2[A]_0 + k_1 e^{(k_1+k_2[A]_0)t}}\right) \tag{3}$$

In eqs 2 and 3, $[A]_t$ and $[B]_t$ are the concentration of A and B at time t, respectively; $[A]_0$ and $[B]_0$ are the initial concentrations of A and B, respectively. Since the 2016 paper reports the HEXRD peak area (PA) the needed equations in terms of PA of the reflections peak for silver metal are derived in section S1 of the SI.

$$PA_t = PA_\infty\left(1 - \frac{k_1 + k_2' PA_\infty}{k_2' PA_\infty + k_1 e^{(k_1+k_2' PA_\infty)t}}\right) \tag{4}$$

PA_t and PA_∞ are the peak areas of Ag^0 reflections at time t and at the end of complete conversion of Ag^+ to Ag^0, $Ck_2' = k_2$, and C is a constant.

The experimental PA versus time data were fit to eq 4 by using nonlinear least-squares fit analysis using OriginPro 8.5 software, which in turn yields the rate constants k_1 and k_2' for the slow, continuous nucleation and autocatalytic surface growth, respectively. Error bars cited come from the fit. Note that we know from published experience[14] that, even if the nucleation step is bimolecular, one can still employ fits to the FW two-step unimolecuar nucleation mechanism because [A] is effectively constant (= $[A]_0$) to a high degree during the induction period, so that k_1 from the unimolecular FW two-step mechanism is related to $k_{1(obs)bimol}$ by the simple relationship $k_1 = k_{1(obs)bimol}[A]_0$, as our 2014 paper addresses in detail.[14] Restated, even if the true nucleation step is bimolecular (or higher molecularity), use of the unimolecular FW two-step mechanism (eqs 1−4 herein) is still mathematically proper as detailed in our 2014 paper.[14]

The peak area versus time experimental data for the growth *rate* were, on the other hand, fit to eq 5, derived in the SI from eq 6,[23] which also yields the rate constants k_1 and k_2' for the slow, continuous nucleation and autocatalytic surface growth, respectively, of the nanoparticle formation reaction.

DOI: 10.1021/acs.jpcc.7b06323
J. Phys. Chem. C 2017, 121, 27643−27654

$$\frac{d[PA]}{dt} = k_1 PA_\infty \cdot e^{(k_1 + k_2' PA_\infty)t} \cdot \left(\frac{k_1 + k_2' PA_\infty}{k_2' PA_\infty + k_1 e^{(k_1 + k_2' PA_\infty)t}} \right)^2 \quad (5)$$

$$\frac{d[B]_t}{dt} = k_1 [A]_0 \cdot e^{(k_1 + k_2 [A]_0)t} \cdot \left(\frac{k_1 + k_2 [A]_0}{k_2 [A]_0 + k_1 e^{(k_1 + k_2 [A]_0)t}} \right)^2 \quad (6)$$

For simulation of the kinetics, the same equations were used in OriginPro 8.5 Version but in the case of simulations by inputting k_1, k_2', and PA_∞ as fixed parameters. An extra significant figure in the curve-fit-obtained k_1 and k_2' values has been deliberately retained to minimize round-off or propagation errors in any subsequent use of those rate constant values.

The errors provided are, again, the errors of the fits, not standard deviations of multiple, separate/repeat experiments. We have known for some time and have published that (i) the errors in k_1 are the largest (and compared to much smaller errors in k_2) and (ii) that the intra-investigator error in at least our own studies of Ir(0) nanoparticle formation are ~50% in k_1, while the inter-investigator error in k_1 is $\sim 10^{1.2}$ over a 7 year period by multiple researchers (see p. 10 304 elsewhere);[24] Experimental reasons (water; trace impurities in acetone solvent in that case;[25] small variations in the amount of free $Ir(1,5\text{-COD})^+$ that is a key species in the nucleation[14,25] (in that case), and other experimental factors are part of the sensitivity of the nucleation rate constants—that are notoriously hard to measure.[4,14,26] In addition, we have recently shown mathematically that k_1 and k_2 (and $[A]_0$) all contribute to each of the key sections of sigmoidal kinetics curves fit by the two-step mechanism; for example, both k_1 and k_2 contribute to the induction period (i.e., and not just k_1 as one might have guessed intuitively).[23]

RESULTS AND DISCUSSION

Proposed Balanced Reaction. For the synthesis of Ag^0_n nanoparticles from the polyol reduction of silver nitrate in the presence of PVP, the first thing one needs is an at least proposed balanced reaction, as given in eq 7.

$$AgNO_3 + \frac{1}{8}HOCH_2CH_2OH + bPVP + \frac{1}{4}H_2O \xrightarrow{130-180\,^\circ C,\ \text{microwave heating}} \frac{1}{n}[Ag^0_n(NO_3^-)_{nx}(PVP)_{nb}] + (1-x)NO_3^- + H^+ + \frac{1}{8}HO_2CCO_2H \quad (7)$$

There is little doubt based on prior literature that the Ag^0_n nanoparticles are formed by well-precedented alcohol-mediated reduction (more generally known as a polyol reduction)[27−30] and then stabilized by PVP polymer and probably surface-adsorbed NO_3^- anions,[31] as eq 7 suggests. Eq 7 further illustrates that trace water is likely a component of the reaction,[32] depending on the level of oxidation of the ethylene glycol reductant—written somewhat arbitrarily above to show its oxidation all the way to oxalic acid, HO_2C-CO_2H (i.e., with full awareness that the initial product derived from ethylene glycol oxidation should be glycol aldehyde, $HOCH_2CHO$, with glycolic acid then being another possible intermediate product, $HOCH_2CO_2H$, en route to the full oxidation product oxalic acid, HO_2CCO_2H). Although balanced reaction stoichiometry was not unequivocally established, nor proposed, previously,[1] for the purposes of the present contribution, eq 7 will suffice. Eq 7 also teaches the additional kinetics studies that could be done by any interested parties, notably determining any kinetic dependence on added H_2O, H^+ product, or ethylene glycol oxidation intermediates, glycol aldehyde, $HOCH_2CHO$, and glycolic acid, $HOCH_2CO_2H$. Such studies are not the purpose, nor necessary, for the present work, which strives to put the prior kinetics data and analysis of the interesting data in the 2016 paper on a firmer, literature-aware, proper kinetics and mechanistic footing, vide infra.

Curve-Fitting the Ag(111) Kinetics Data to the FW Unimolecular Nucleation Two-Step Mechanism. The peak area data of Ag(111) and Ag(200) reflections reported in the 2016 paper[1] were used directly as described in the Experimental Section. To start, the full data as originally given[1] were used, that is, including the first ~5−6 min where heating is occurring as well. The data obtained from the Ag(111) reflections in Figure A of the 2016 paper[1] are well-fit, as shown in Figure 2a, to the FW two-step mechanism[15] consisting of slow, continuous nucleation (A → B, rate constant k_1) and autocatalytic surface growth (A + B →2B, rate constant k_2), eq 1, where again A stands for the Ag(I) precursor and B for the growing Ag^0_n nanoparticles. The fit in Figure 2a yields the rate constants $k_1 = (1.4 \pm 0.1) \times 10^{-4}$ min^{-1}, $k_2' = (2.84 \pm 0.04) \times 10^{-2}$ (au)$^{-1}$ min^{-1} along with a reduced Chi-Sqr = 1.30×10^{-2}, and $R^2 = 0.99946$. The relatively large value of $k_2'/k_1 = 200$ (au)$^{-1}$ indicates a relatively high level of kinetic control for the formation of the Ag^0 nanoparticles[33] (i.e., and in the range of peak area values experimentally observed herein at the end point, that sum to between ~5−12 au that, then, can be multiplied by the $k_2'/k_1 = 200$ (au)$^{-1}$ to give a unitless, then here $k_2' \cdot au/k_1 = 1000-2400$, value).

The resultant k_1 and k_2' values obtained using eq 4 were then combined with the peak area value PA_∞ (i.e., when the Ag^+ ion is completely converted to Ag^0)[1] to simulate the growth rate vs time using eq 5 and to compare it to the experimentally determined value (Figure S4 from the Supporting Information of the 2016 paper[1]). Figure 2b shows that simulation coplotted over the experimental data, revealing that both the experimental growth-rate curve is largely accounted for, albeit with the simulation showing a slight time delay of about 3 min that will be dealt with in a moment.

We also performed the reverse fit and simulation. First we fit the experimental growth-rate data using eq 5 to the FW two-step mechanism,[15] efforts that resulted in a close fit (Figure S1a in the SI) and the rate constants $k_1 = (2.1 \pm 0.3) \times 10^{-4}$ min^{-1}, $k_2' = (2.87 \pm 0.06) \times 10^{-2}$ (au)$^{-1}$ min^{-1}, so a k_1 was obtained that was slightly different from the one obtained above by the reverse fitting in Figure 2a, $k_1 = (1.4 \pm 0.1) \times 10^{-4}$ min^{-1}, but k_2 values obtained from both fits are identical within the stated errors. Next, we simulated the experimental PA versus time data using those eq 5-fit-obtained rate constants by placing them into eq 4, Figure S1b in the SI. The resultant simulated PA growth-rate curve matches the experimental data, but again slightly shifted in time to the left (Figure S1b in the SI).

These above two fits and simulations led, empirically and in turn, to the notion of deliberately dropping the first ~3 min where the heating ramp is not yet near ~140 °C. Performing the same two fittings and simulations, but now with the first 3 min of the (heating lag-time data) deliberately omitted, yielded Figure 2c (for fitting the PA versus time data), which shows an excellent fit to the FW two-step mechanism,[15] and resultant rate constants $k_1 = (4.0 \pm 0.3) \times 10^{-4}$ min^{-1} and $k_2' = (2.83 \pm$

DOI: 10.1021/acs.jpcc.7b06323
J. Phys. Chem. C 2017, 121, 27643−27654

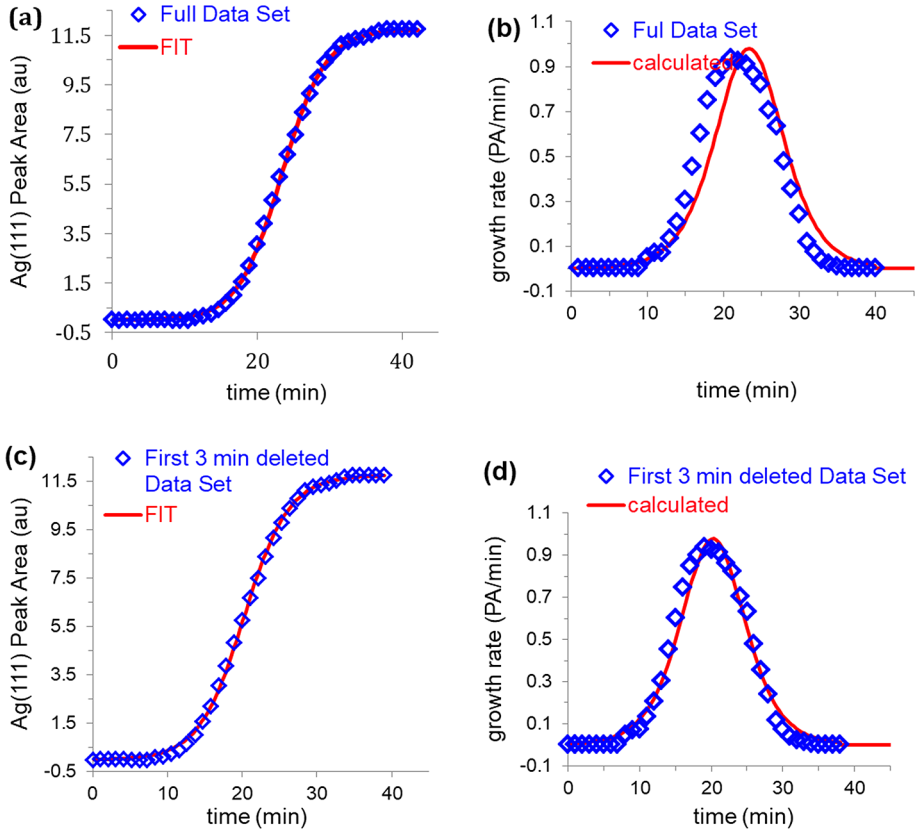


Figure 2. (a) Peak area versus time plot (obtained from the peak area of Ag(111) reflections in Figure 2A of the 2016 paper[1]) in the course of the $Ag^+ \rightarrow Ag^0$ reaction at 140 °C and its fit to the FW two-step mechanism[15] yielding $k_1 = (1.4 \pm 0.1) \times 10^{-4}$ min^{-1}, $k_2' = (2.84 \pm 0.04) \times 10^{-2}$ $(au)^{-1}$ min^{-1} with a reduced Chi-Sqr = 1.35×10^{-2}, and $R^2 = 0.99946$. (b) Simulation of the experimentally determined growth-rate variation with time given in Figure S4 in the Supporting Information of the 2016 paper,[1] using the rate constants obtained in (a). (c) The same peak area versus time plot as in (a) but with the first 3 min deleted and its fit to the FW two-step mechanism[15] yielding $k_1 = (4.0 \pm 0.3) \times 10^{-4}$ min^{-1}, $k_2' = (2.83 \pm 0.04) \times 10^{-2}$ $(au)^{-1}$ min^{-1} with a reduced Chi-Sqr = 1.35×10^{-2}, and $R^2 = 0.99946$. (d) Simulation of the experimentally determined growth-rate variation with time given in Figure S4 in the Supporting Information of the 2016 paper,[1] using the rate constants obtained in (c). Notable here is that (i) the fit to the FW two-step mechanism adequately accounts for the kinetics data and (ii) that the better fit to the FW two-step mechanisms in 2d vs 2b is evidence supporting the deliberate deletion of the first ~3 min of kinetics data, during which heating of the solution is occurring.

$0.04) \times 10^{-2}$ $(au)^{-1}$ min^{-1} with a reduced Chi-Sqr = 1.35×10^{-2}, and $R^2 = 0.99946$. The simulation of the growth-rate data using these rate constant values as fixed input parameters and eq 5 gives, now, an even better match to the experimental plot as shown in Figure 2d. The reverse fitting was also performed, yielding an excellent fit now to the growth-rate data (Figure S1c in the SI) and the rate constants $k_1 = (4.0 \pm 0.5) \times 10^{-4}$ min^{-1} and $k_2' = (2.87 \pm 0.06) \times 10^{-2}$ $(au)^{-1}$ min^{-1}, values are very close to the values obtained from the fit of PA versus time data in Figure 2c. Pleasingly, the simulation of peak area versus time data from these resultant rate constants and the PA_∞ gives an excellent match to the experimental PA versus time data, Figure S1d of the SI.

Taking the above results all together allows us to suggest that the FW two-step mechanism[15] provides a very good, deliberately minimalistic description of the formation of Ag^0 nanoparticles via polyol reduction of Ag(I) ions in the presence of PVP stabilizer and driven by microwave heating to 140 °C. As a result, clarified greatly are the prior author's word-only claims of "continuously formed seeds" and a "typical self-catalytic" reaction, kinetically and mechanistically imprecise concepts that can now be replaced by the rigorously defined, as well as curve-fit supported, concepts from the FW two-step mechanism of slow, continuous nucleation followed by fast, autocatalytic surface growth.[15]

Note also that the prior claim[1] that "stable nuclei called seeds" are formed is imprecise and arguably incorrect, as the most recently available evidence is that "seeds" are not formed as classical nucleation theory postulates. Instead, a small, kinetically effective nucleus (KEN) of just 2−3 atoms now has growing precedent.[13,14] Moreover, that KEN typically does not build up but, instead, is quickly consumed in the fast, autocatalytic growth step—concepts far removed from the notion of the claimed "stable seeds" based on seeing[1] what are really the first observable clusters[14] of ~9.9 nm. Another important point here is that ~9.9 nm $Ag(0)_n$ nanoparticles are already rather large and contain ~3×10^4 Ag(0) atoms—so nucleation, growth, and, one would expect, some agglomeration (aggregation; coalescence) have been ongoing for some time before the "seeds" are detectable by HEXRD.

Curve-Fitting the Ag(200) Kinetics Data to the FW Unimolecular Nucleation Two-Step Mechanism. The experimental peak area data collected for the Ag(200) reflections in Figure 2C of the 2016 paper[1] (at 140 °C with microwave heating[1] of the polyol reduction of Ag^+ in the presence of PVP stabilizer) were plotted versus time in Figure 3 (blue diamonds). That peak area versus time data (without omitting the first 3 min) for the peak area of Ag(200) reflections are also well-fit by the FW two-step mechanism[15] as displayed in Figure 3 (red line), yielding $k_1 = (1.9 \pm 0.3) \times$

DOI: 10.1021/acs.jpcc.7b06323
J. Phys. Chem. C 2017, 121, 27643−27654

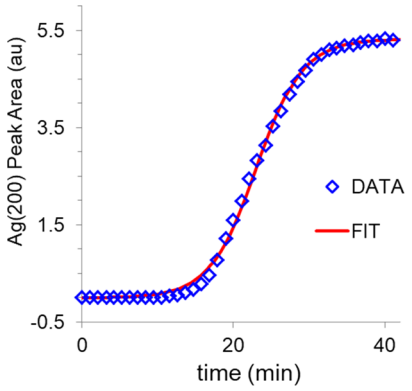


Figure 3. Ag(200) peak area versus time plot (obtained from Ag(200) reflections in Figure 2C of the 2016 paper[1]) in the course of the $Ag^+ \rightarrow Ag^0$ reaction at 140 °C and its fit to the FW two-step mechanism[15] yielding $k_1 = (1.9 \pm 0.3) \times 10^{-4}$ min^{-1}, $k_2' = (6.08 \pm 0.13) \times 10^{-2}$ $(au)^{-1}min^{-1}$. Reduced Chi-Sqr = 6.55×10^{-3}, $R^2 = 0.99866$.

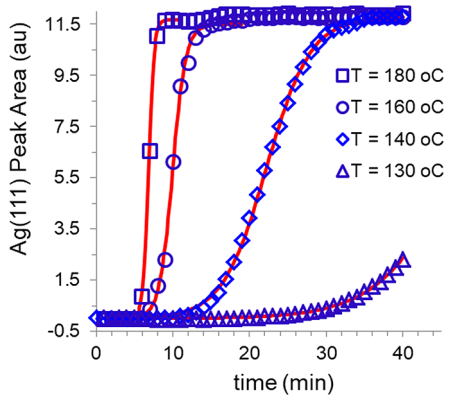


Figure 4. Ag(111) peak area versus time plots obtained from the peak area of Ag(111) reflections at four different temperatures produced via microwave heating (Figure 3A in the 2016 paper[1]). The data from all four different temperatures is well-fit by the FW two-step mechanism,[15] yielding the k_1 and k_2' rate constants values and associated fitting statistics summarized in Table 1.

10^{-4} min^{-1}, $k_2' = (6.08 \pm 0.13) \times 10^{-2}$ $(au)^{-1}min^{-1}$ (reduced Chi-Sqr = 6.55×10^{-3}, $R^2 = 0.99866$). This is an important result, one that builds off the novel data and powerful physical methods employed in the valuable 2016 paper that are a compliment to experimental abilities and efforts of the prior authors.[1]

The rate constants for the Ag(111) data are $k_1 = (1.4 \pm 0.1) \times 10^{-4}$ min^{-1} and $k_2' = (2.83 \pm 0.04) \times 10^{-2}$ $(au)^{-1}$ min^{-1}, and for the Ag(200) data are $k_1 = (1.9 \pm 0.3) \times 10^{-4}$ min^{-1} and $k_2' = (6.08 \pm 0.13) \times 10^{-2}$ $(au)^{-1}$ min^{-1}; rate constants obtained herein for the first time from the HEXRD data. However, using the resultant rate constants and eq 4 to try to fit the relative peak areas, PA_{111}/PA_{200} vs time plotted in Figure 2D of the 2016 paper[1] reveals that while the data past 18 min in that plot is well accounted for, the data before 18 min are not; see Figure S2 of the SI of the present paper. The results from the present analysis and those shown in Figure S2 of the SI suggest that there is likely a large error in the PA_{111}/PA_{200} peak area ratio data for the first ~18 min. A large error likely results because the initial PA_{200} peak area is small, near zero early on with associated relatively large error bars, and the PA_{200} value is in the denominator of the peak-area-ratio expression—a resulting too large PA_{111}/PA_{200} peak area ratio resulting with large error bars. Unfortunately, the experimental or estimated error bars for the PA_{111}/PA_{200} peak area ratio data were not provided[1] but are crucial to being able to interpret that peak-area-ratio correctly—whether the Ag(111) and Ag(200) grow in parallel, sequential, or perhaps a combination of parallel and sequential reactions (among other conceivable mechanisms), a point discussed more in the SI along with Figure S2 there. In short, the more intimate mechanism for formation of the Ag(111) and Ag(200) facets is not apparent at this time from the available data. It is likely that at least the k_2' values are composites for formation of a combination of the Ag(111) and Ag(200) peak areas, even though they were measured separately and directly for those individual facets—a mathematical subtlety of parallel reaction kinetics discussed more along with Figure S2 of the SI for the interested reader.

Temperature Dependence of the Ag(111) Peak Area Kinetics Data. The kinetics data collected from the peak area of Ag(111) reflections at four different temperatures with microwave heating (Figure 3A in the 2016 paper[1]) were plotted versus time in Figure 4. All the data at four different temperatures are well-fit by the FW two-step mechanism,[15] Figure 4 yielding the desired k_1 and k_2' rate constants as well as the least-squares correlation parameters, Table 1.

A look at the temperature-dependent rate constant data in Table 1 reveals some precedented, and therefore not unexpected, trends:[34] the better defined, less noisy k_2' rate constants increase with increasing temperature as expected, but the nucleation rate constants k_1, which are notoriously hard to measure precisely,[14,15] do not—for example, the lower temperature 140 °C k_1 value is ostensibly larger than the higher temperature, 160 °C k_1 value. Therefore, a meaningful Arrhenius, $\ln(k)$ versus $1/T$, plot could be constructed for only the growth-rate constant, k_2', Figure 5. An activation energy of $E_a = 83 \pm 2$ kJ/mol (19.8 ± 0.5 kcal/mol). Note that the present kinetically rigorous analysis teaches that, unfortunately, a reliable A factor and corresponding $\Delta S^{\ddagger}$ is not available in any meaningful standard state, because the needed complete mass balance and the total peak areas (PAs) of the Ag(111), Ag(200) plus Ag(220) are not available,[1] values that are required for the conversion of the PAs to their corresponding converted $[Ag^+]$, and formed $[Ag^0]$, values and, hence, also for the value of C in $k_2' = k_2/C$. It is easily shown that this means that the A value and associated $\Delta S^{\ddagger}$ will be off by that (unknown) constant; for example, the intercept of a $\ln k_2'$ vs $1/T$ plot being: intercept = $\ln A + \ln C$ (that intercept = 16.4 in Figure 5).

Importantly, the E_a obtained herein updates the claim in the 2016 paper[1] that "the formation of seeds..." (i.e, the ~9.9 nm particles) occurs "with activation energy of 20.34 kJ/mol" (= 4.86 kcal/mol). This reported value and its assignment to "seed formation" can now be seen to be (i) at best unclear if not confused conceptually, because the required specific balanced chemical equation needed to define the reaction that the E_a refers to was not provided;[1] (ii) to be in error numerically relative to the now well-defined steps of nucleation and autocatalytic surface growth of the Ag^0 nanoparticles, steps not separated kinetically previously;[1] and also (iii) not to make much physical sense because the E_a = 4.86 kcal/mol value obtained is too low to be correct for either of the nucleation or growth steps of the polyol reduction of Ag^+ ion, a reaction known to occur only at temperatures higher than 100 °C,[35] and a reaction that occurs in the present study only once one is

DOI: 10.1021/acs.jpcc.7b06323
J. Phys. Chem. C 2017, 121, 27643−27654

Table 1. k_1 and k_2' Rate Constants for the Nucleation and Autocatalytic Surface Growth, Respectively, of Ag(0) Nanoparticles According to the Ag(111) Data[a]

T (°C)	k_1 (min^{-1})	k_2' ($(au)^{-1}$ min^{-1})	χ^2	R^2
180	$(1.3 \pm 0.6) \times 10^{-8}$	$(24.1 \pm 0.6) \times 10^{-2}$	2.68×10^{-3}	0.99991
160	$(1.1 \pm 0.6) \times 10^{-5}$	$(10.1 \pm 0.6) \times 10^{-2}$	5.19×10^{-2}	0.9982
140	$(1.5 \pm 0.1) \times 10^{-4}$	$(2.95 \pm 0.04) \times 10^{-2}$	1.27×10^{-2}	0.9995
130	$(2.0 \pm 0.2) \times 10^{-5}$	$(1.65 \pm 0.02) \times 10^{-2}$	6.75×10^{-4}	0.99812

[a]At four different temperatures and the nonlinear least-square correlation parameters.

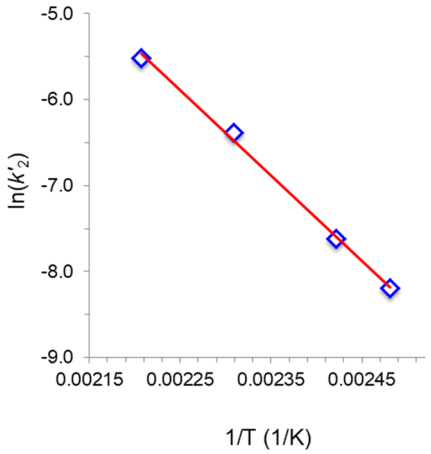


Figure 5. Arrhenius $\ln(k_2')$ versus $1/T$ plot for the autocatalytic surface growth, k_2', step from the polyol reduction of $AgNO_3$ solution in the presence of PVP stabilizer at four different temperatures driven by microwave heating. A linear least-squares fit of the data to the Arrhenius equation yielded $\ln(k_2') = -9933(1/T) + 16.43$, with $R^2 = 0.997$.

≥130−180 °C, all of which hint at E_a values ≫4.86 kcal/mol (and unless the reaction has a hugely negative entropy).

Although no E_a values for Ag^0_n nanoparticle formation from the literature were cited for comparison in the previous study, we did find one value on searching the literature: an $E_{a,composite}$ = 77.9 ± 1.8 kJ/mol (18.6 ± 0.5 kcal/mol). We say composite here because this value reported for the formation of silver nanoparticles from the decomposition of silver acetate does not have nucleation deconvolution from the growth step(s).[36] Nevertheless, that reaction is reported to occur at an appreciable rate at 170 °C, again meaning that the reported[1] E_a value of ≫4.86 kcal/mol is not meaningful physically.[35] That is, the E_a value obtained from the empirical fitting function used previously[1] is, unfortunately, a telling example of what was noted in the Introduction: the hugely insidious, misleading nature of getting empirical parameters, ones therefore not defined properly by balanced chemical reactions, and then trying in vain to attach words and concepts to those values to try to describe what is going on physically, in the present case the putative "formation of seeds" (that are really large, ∼9.9 nm first observable clusters[14] by the HEXRD method) with an unprecedented low E_a = 4.86 kcal/mol that, in all probability, refers to nothing of chemical value.

Effect of Ag(I) Ion Concentration and Stabilizer Concentration on the Formation Kinetics of Ag^0 Nanoparticles. Figures S10 and S11 of the 2016 paper[1] report peak area kinetics data for Ag^0 nanoparticle formation as a function of varying the initial concentrations of $AgNO_3$ or PVP stabilizer (as before in ethylene glycol solution, at 140 °C achieved via microwave heating). The peak area kinetics data in Figures S10 and S11 of the 2016 paper[1] were displayed as part of the present re-analysis as Figures S3 and S4 for the experiments varying the initial [$AgNO_3$] and [PVP] stabilizer, respectively. As Figures S3 and S4 show, each of the six separate kinetics curves are again well-fit by the FW two-step mechanism.[15] Hence, we can conclude at this point that the FW two-step mechanism is able to account quantitatively for all the kinetics data in the 2016 paper.[1] The resultant k_1 and k_2' rate constants are summarized in Table 2.

Again not unexpectedly, the hard-to-measure-precisely[14,15] nucleation rate constant k_1 have scattered values. Interestingly, the typically better defined[5−7] k_2' rate constant for autocatalytic surface growth remains unaltered with the increasing concentration of PVP stabilizer, but decreases with the increasing initial concentration of Ag(I) ion, a find that pleasingly supports the prior author's statement that "increasing the concentration of $AgNO_3$...only slightly slows the reaction kinetics."[1]

The mechanistic insights here are multiple and interesting, namely that (i) the mechanism is more complex—in the case of these very large ∼100 nm $Ag(0)_n$ nanoparticles, much more complex—than the by-design minimalistic FW two-step mechanism (as will almost always be the case, as noted elsewhere).[6,14] However, several published examples compellingly demonstrate that fits to the FW two-step mechanism can provide a very valuable, often required, first mechanistic foundation from which to discover the more complex, underlying mechanisms.[8,37−40] For example, (ii) one possible

Table 2. k_1 and k_2' Rate Constants for the Formation of Ag^0 Nanoparticles at 140 °C[b]

[Ag^+] (M)	[PVP] (M)	k_1 (min^{-1})	k_2' $(au)^{-1}$ min^{-1})	χ^2	R^2
0.1	[a]	$(4.3 \pm 3.6)\times10^{-7}$	$(24.5 \pm 1.5)\times10^{-2}$	1.35×10^{-2}	0.9979
0.2	[a]	$(2.2 \pm 0.8)\times10^{-5}$	$(9.15 \pm 0.36)\times10^{-2}$	3.57×10^{-2}	0.9985
0.3	[a]	$(8.5 \pm 5.7)\times10^{-7}$	$(7.73 \pm 0.39)\times10^{-2}$	9.19×10^{-2}	0.9984
[a]	0.2	$(2.5 \pm 1.4)\times10^{-5}$	$(9.00 \pm 0.53)\times10^{-2}$	8.19×10^{-2}	0.9965
[a]	0.3	$(2.4 \pm 0.8)\times10^{-5}$	$(9.06 \pm 0.32)\times10^{-2}$	3.02×10^{-2}	0.9987
[a]	0.4	$(5.5 \pm 2.8)\times10^{-5}$	$(8.20 \pm 0.47)\times10^{-2}$	8.77×10^{-2}	0.9964

[a]These PVP concentrations were kept constant, but that specific value was not reported in the 2016 paper.[1] [b]As a function of various starting concentrations of the Ag(I) ion and PVP stabilizer, plus the resultant nonlinear least-square parameters for the fits to the FW two-step mechanism.

DOI: 10.1021/acs.jpcc.7b06323
J. Phys. Chem. C 2017, 121, 27643−27654

explanation for inverse dependence of k_2' on the starting [$AgNO_3$] is a prior equilibrium in which ion-paired silver nitrate in ethylene glycol reversibly dissociates to its component ions, the freely diffusing Ag^+ being more oxidizing and hence more reactive, $Ag^+NO_3^- \leftrightarrows Ag^+ + NO_3^- \rightarrow$ to further, on-path reaction(s). Another possibility is that, in ethylene glycol, a silver nitrate aggregate is present that dissociates to what one then postulates is the more reactive monomer, for example, something such as $(AgNO_3)_n \leftrightarrows nAgNO_3 \rightarrow$ to further, on-path reaction(s). Additionally, the present work generates the insight that (iii) the k_2' step must be a composite of elementary steps and, hence, should be labeled as $k_{2,\text{apparent}}'$ to make that clear; and that (iv) the activation energy E_a value for the k_2' step is, also and therefore, a composite that should be labeled $E_{a,\text{apparent}} = 83 \pm 2$ kJ/mol (19.8 ± 0.5 kcal/mol) to make that point clear as well. None of the above insights were possible from the prior fitting to an empirical function.[1] A fit to the two-step mechanism begins the journey to the true, underlying mechanism, even if just "inch-wise" as is the evolutionary, disproof-based, and hence often slow and tedious nature of reliable mechanistic work.

Additional Insights into What Is Occurring Physically and Mechanistically vs the Words and Concepts Disconnected from the Empirical Function That Were Used Previously. As discussed in the Introduction, there is a huge, insidious problem in studies of chemical reactions and their mechanisms that fail to use well-defined chemical equations and the rate constants as well as proper chemical terms they define—such as A → B, rate constant k_1, for slow continuous nucleation, and A + B → 2B, rate constant k_2', for autocatalytic surface growth. That insidious problem is the highly misleading, confusing disconnect that then unavoidably occurs in measured rate parameters (that are NOT rate constants, because they do not refer to balanced chemical reactions) and especially in the words and concepts adapted from the literature in a hit and miss way to try to describe the observed results physically and mechanistically.[6,7] Summarized and addressed next are the misleading, mechanistically and physically incorrect words and concepts that resulted from the prior use of an empirical fitting function.[1]

The terms and concepts used previously,[1] which have no connection to the equations used to fit the kinetics, and which can now be replaced and re-conceptualized by the results presented herein, include: (a) the claim of a "supersaturated concentration of Ag^0 atoms", despite the fact that prior literature notes that single, metal-zero, naked atoms are likely NOT involved in nucleation;[13−15,18] (b) the claim that "the formation of seeds follows typical first-order reaction kinetics"—and "with activation energy of 20.34 kJ/mol"—is shown herein to be at least misleading, the formation of ∼9.9 nm "seeds" actually including many cycles of an autocatalytic growth step if not probably also agglomeration. Additionally, evidence is accumulating that nucleation is often second-order,[13,14] not first-order in metal precursor. Furthermore, (c) the claim that "there are two different types of reaction kinetics" is at best unclear ("what two types of kinetics"?), and shown herein to be misleading, because a single, well-precedented kinetics scheme of the FW two-step mechanism is able to quantitatively account for all the prior kinetics and over each of the full kinetics curves, vide supra; (d) the imprecise claim of a "typical self-catalytic reaction mechanism" can now be replaced with the precisely defined concept of autocatalytic surface growth, a well-precedented concept for over 20 years now;[15] and (e) the claim that the first-seen ∼9.9 nm clusters are "seeds" can now be better understood as what have been termed the "first observable clusters".[14] Additionally, (f) the claim in the Abstract of the 2016 paper that "the microwave synthesis of Ag nanoparticles proceeds with reaction kinetics significantly different from the synthesis present in conventional oil heating" is poorly supported. In fact, the most commonly used nanoparticle formation mechanism when conventional heating is used,[3−18] namely the two-step kinetics scheme employed herein, is able to fit all of the reported kinetics data[1] as well as that of several other Ag^0_n formation systems.[8−11] Finally (g) the prior claim[1] that the synthesis includes "four well-separated steps,... incubation of the nucleation process, formation of seeds, growth of seeds, and completion of the reaction" is poorly defined physically and unsupported kinetically—the "completion of reaction" perhaps being agglomeration, vide infra. In point of fact, the FW two-step mechanism (or its two-step agglomeration counterpart, vide infra) is all that has been needed to fit the observed kinetics of all of the primary kinetics curves provided previously.[1] Hence and while the claim of "4 stages" seems on one hand to be reasonable, this claim is not mechanistically rigorous because it is not supported by any corresponding kinetics scheme, associated equations used to fit the data, nor resultant rate constants.

However, it is important to give the prior study credit for noting the broad range of particles formed and for their attempt to interpret this, specifically their statement suggesting that "the Ag nanoparticles coalescence, ...via possible orientated attachment and fusion". We can reframe what the authors were hinting at in terms of the precedented agglomeration steps of the highly disproof-based four-step mechanism:[6,12] namely bimolecular agglomeration (B + B → C; rate constant k_3) followed by autocatalytic agglomeration (B + C → 1.5 C; rate constant k_4), where C is the growing, average, agglomerated particle. Interestingly, Figure S5 of the SI demonstrates that just the two-step bimolecular agglomeration plus autocatalytic agglomeration mechanistic formulation given above fits the data in the 2016 paper. This is not surprising, however, because the underlying integrated kinetics equation is basically mathematically identical to that for the two-step nucleation and autocatalytic growth mechanism, except for the different 1.5 stoichiometry factor and that B and C are present rather than A and B.

These results, in turn, lead one to realize an important ambiguity in the 2016 paper (one that unavoidably also carries over to the present re-interpretation of that work; see the SI for additional discussion): it is not clear from the 2016 paper what one is actually starting with for the purposes of the HEXRD monitoring of crystalline Ag(111) and Ag(200) formation that "starts" with "seeds" that contain ∼3×10^4 Ag(0) atoms and ends up in ∼100 nm particles. Is Ag^+ (="A") really the proper starting point conceptually (i.e., and for the HEXRD monitoring), or are nucleation and surface autocatalytic growth fast at the ≥140 °C temperatures employed, *so that it is actually Ag^0_n preformed by the hot ethylene glycol (i.e., really Ag^0_n = "B") that one is truly "beginning with" in the microwave synthesis en route to the final, HEXRD-observed, crystalline Ag(111) and Ag(200), 0.1 μm-sized products?* Put another way, the actual starting material for the purposes of the kinetics analysis is a large uncertainty in the 2016 study, one made apparent as part of the present studies and re-analysis. The SI presents more on this interesting, nontrivial issue and its possible implications for

DOI: 10.1021/acs.jpcc.7b06323
J. Phys. Chem. C 2017, 121, 27643−27654

the interested reader. Hence, and even though the prior was on track for noting that "coalescence" was probably involved in their reaction, the problem is because no guidance results from the empirical function used to fit the kinetics, the prior work imprecisely calls what they are monitoring (e.g., in the paper's Abstract) "nucleation and growth" and "the formation of seeds (nucleation)" and "the growth of seeds (growth)". Associating "nucleation" with 9.9 nm first observable clusters that already contain $\sim 3 \times 10^4$ atoms is not physically meaningful and is, in fact, misleading. This type of confusion results completely and "automatically" if one's kinetics and mechanistic treatment does not contain the balanced reactions required to define rigorously the kinetics, their associated rate constant, and the well-defined concepts and words that one is then "allowed" to use to describe the chemistry physically. Note also here that if the actual species being monitored by the HEXRD is primarily the agglomeration of already formed Ag^0_n clusters, then the correct reactions, rate constants, and proper concepts and words will be significantly different.

In short, there is a nearly complete disconnect in the prior work[1] between the elegantly and expertly obtained, very valuable, novel kinetics data—superb data at a level of detail that monitors the separate Ag(111) vs the Ag(200) facets—and the words and concepts used to attempt to describe what is occurring mechanistically and hence physically. Such a disconnect is unfortunately far too common;[6,7] it results from attempting to use empirical, nonrigorous-mechanism-derived equations for the fitting of kinetics data, which in turn invariably results in the poor choice of improper, unconnected concepts and words to describe what is occurring mechanistically and physically—thereby generating and propagating confusion in the resultant literature. *It is a practice that must be abandoned!* Providing evidence against this practice is a main reason why we have taken time to reanalyze the present, again elegantly and expertly obtained[1], kinetics data for the formation of Ag(111) and Ag(200) facets under the interesting microwave heating, and polyol reduction, conditions employed. The data is spectacular! It deserves as good an analysis as possible, one done in full awareness of the known kinetics and mechanistic literature of nanoparticle nucleation, growth, and agglomeration.

SUMMARY AND CONCLUSIONS

In summary, some insights and conclusions from the present contribution are that

(1) The well-established principle of sound science—that you must go to and learn what the prior literature has to say that is relevant to your problem—is once again emphasized. Disproof of multiple alternative hypotheses is also crucial,[41] for example, the hypotheses relevant to the present example that the FW two-step mechanism can account for the formation of very large nanoparticles, or the hypothesis that preformed nanoparticles, B, should really be the true starting material for the kinetics in the 2016 paper.

(2) The very valuable, elegantly and expertly obtained, kinetics data in a 2016 paper, resolving the rates of formation of Ag(111) and Ag(200) facets, has been critically re-analyzed herein in light of the extant, now extensive, relevant literature of the kinetics and mechanisms of nanoparticle nucleation, growth, and agglomeration plus other relevant literature.[3−18]

(3) It has been shown that all of the kinetics curves in the 2016 paper[1] can be quantitatively accounted for by the now 20 year-old, 1997 FW two-step mechanism[15] of slow continuous nucleation (A → B, rate constant k_1), then fast autocatalytic surface growth (A + B → 2B, rate constant k_2, or in the present case, k_2'), where A is Ag^+ and B is Ag^0_n. What especially the resultant k_2' rate constant means, and how to interpret it, are another issue, one discussed further in the SI.

(4) The analysis of the kinetics data by the highly disproof-based, hence kinetically and mechanistically rigorous, FW two-step mechanism does provide well-defined concepts and precise words to describe the extant reaction chemically and physically: slow, continuous nucleation, and autocatalytic surface growth—that is, assuming that the HEXRD is monitoring the conversion of Ag^+ ("A") in to Ag^0_n ("B") as believed in the 2016 paper.

(5) On the other hand, it is likely that agglomeration steps that are part of the four-step mechanism[4,6,12] are present, given that the final particle distribution is relatively broad. Hence, if Ag^0_n nanoparticles are quickly preformed under the (high temperature) reaction conditions (i.e., and from relatively easily reduced Ag^+), so that one is really starting with "B" = Ag^0_n and not "A" = Ag^+ for the purposes of the kinetics (and so that the B + B → C, then B + C → 1.5 C formalism should be used to analyze the kinetics and as Figure S5 of the SI shows will fit the data), then the prior work needs to be reformulated rather completely. In addition, if B is the true starting material, then everywhere herein where "nucleation and autocatalytic surface growth" formation of nanoparticles is used, then those terms would need to be replaced by "bimolecular nucleation of agglomeration" and "autocatalytic agglomeration of nanoparticles". "Know thy reactants and thy products" is a well-known rule of reliable chemical kinetics and mechanism, one attributed to Prof. Ralph G. Pearson.[42] Another key point here, one discussed more in the SI, is that these two possible qualitative, conceptual descriptions of what the HEXRD is actually monitoring are what Prof. J. Platt called "logical boxes" in his classic paper about how science is best done.[41] Providing the conceptual/logical boxes of slow, continuous nucleation and autocatalytic growth, or nucleation of agglomeration and autocatalytic agglomerative growth if those are the main processes present, are the main strength of the by-design, minimal, highly disproof-based, two-step mechanisms cited above and in the present work. That is why the two-step FW mechanism has enjoyed such broad appeal, as documented in the SI for the interested reader.

(6) The present work demonstrates (a) that one needs to avoid using empirical functions that lack any physical meaning to fit such sigmoidal kinetics data when well-defined mechanistic equations and associated functions are available, and (b) that one needs to avoid the kinetically improper, highly misleading practice of just fitting one, somewhat randomly chosen, part of a kinetics curve and then claiming a reaction order relevant to the full kinetics curve.

(7) Evidence has been uncovered suggesting that the PA_{111}/PA_{200} peak area ratio vs time in Figure 2D in the 2016 paper[1] likely has large error bars at short initial times where the PA_{200} is small (closer to zero), so that the

DOI: 10.1021/acs.jpcc.7b06323
J. Phys. Chem. C 2017, 121, 27643−27654

PA_{111}/PA_{200} peak area ratio is inherently imprecisely determined at those low PA_{200} peak area values. This is not in any way a fault of the prior work,[1] rather just an experimental reality of the precision available in even state-of-the-art, synchrotron-based, dynamic HEXRD studies. This uncertainty in the PA_{111}/PA_{200} peak area ratio at short times in turn limits a more detailed mechanistic analysis of how the Ag(111) vs the Ag(200) facets form, for example, in parallel reactions, sequential reactions, or perhaps a combination of both (or perhaps some different mechanism). This ambiguity has the added effect that the underlying components, contributing to especially the k_2' apparent rate constant and perhaps also to the k_1 (then apparent) rate constant, cannot be dissected at this time, as discussed more in the SI along with the associated Figure S2.

(8) (i) Lastly, there is the (remarkable) observation that the two pseudoelementary step mechanism is able to at least fit the kinetics data of the formation of ∼100 nm $Ag(0)_n$ nanoparticles in which $n \sim 10^7$ Ag^+ atoms have been reduced to $\sim 10^7$ Ag(0) atoms in what must have involved $>10^7$ elementary steps. The two pseudoelementary steps of A → B, then A + B → 2 B and the associated averaged, apparent rate constants k_1 and probably especially k_2' have, then, averaged—and in that sense hidden—a huge amount of chemistry that one would like to access with the goal of better understanding. For certain, the hugely composite resultant rate constant k_2 should be interpreted only with considerable caution, especially in comparison to the apparent rate constants obtained from much smaller, ∼10−20 nm particle formation reactions. That caution and caveat so stated, well-designed, careful k_1 and k_2 measurements as a function of smaller to larger nanoparticle formation is of interest and may yield novel insights, a point discussed more in the SI. In the present example and because the final Ag^0_n nanoparticles are so large, the resultant especially k_2 rate constant becomes averaged over such a large surface-area change and resultant scaling factor[15] (designed to compensate for that changing number of surface vs total atoms), that k_2 becomes relatively imprecise and hard to know how to interpret, at least presently. The SI discusses this point as well in greater detail for interested reader. We thank Dr. Y. Sun for bringing this point to our attention.

(ii) As for the k_1 value, it will be very interesting to compare k_1 values for such large, ∼100 nm, and much smaller, ∼10−20 nm, nanoparticles of the same metal (and where those rate constants are obtained under conditions as identical as possible as the formation of different-size nanoparticles will allow). The interesting, presently untested prediction from our recent work on nucleation[13,14] is that the k_1 values will more generally reflect low molecularity nucleation and, therefore, tend to be both more valid and less variable, if not "relatively constant", over even very different sized nanoparticles (and at least in comparison to the anticipated larger changes in k_2 as a function of increasing nanoparticle size).

Finally, for readers interested in either these specific results or the use of the FW two-step[15] and subsequent four-step[4,6,12] kinetic models of nucleation, growth, and two types of agglomeration, they are referred to the detailed discussions elsewhere of the strengths, and *especially the caveats and weaknesses*, of these disproof-based, deliberately minimalistic, Ockham's razor obeying, kinetics models.[14] The weaknesses in general result from the minimalistic, too-simple nature and the averaged values (e.g., the above-noted average rate constants and average size of nanoparticles[5]) that result from the two-, three-, or four-step kinetics models.

The weaknesses of the two- and four-step models so noted, the reader is also directed to the growing list of examples[8,37−40] demonstrating that the composite, pseudoelementary[13−15] steps of A → B, and A + B → 2B (or B + B → B, and B + C → 1.5C) contain sums of the underlying, more detailed, intimate chemical mechanism and truly elementary steps that one can then tease out in at least simpler and favorable cases with additional work. Indeed, in one exemplary case a fit to the pseudoelementary two-step model A → B, and A + B → 2B allowed the discovery of the identity of the hidden catalyst, B, and then the underlying catalytic cycle.[39] Important to note is that all other, prior attempts to uncover the catalyst and associated mechanism had failed, even in the hands of a world-class mechanistic group at a top university because of the complexity of the reaction and its autocatalytic component.[39] The discovery of the underlying mechanism required, first, a fit to the two-step model. This example is significant in a way that is difficult to overemphasize, namely the mechanistically powerful application of nonempirical kinetics models to help dissect complex, multistep reactions into their underlying elementary-steps by, first, fits to minimalistic mechanisms composed of pseudoelementary steps.[15]

An important take-home message, then, is that even just starting with pseudoelementary steps such as A → B and A + B → 2B to account for the observed sigmoidal kinetics, those deliberately simplified but precise, balanced chemical equations provide the thereby first-available, associated, precisely defined words and concepts that one can then use to describe reliably the chemistry properly, mechanistically and physically. Average rate constants for those well-defined chemical processes also result, although they are inherently averaged, composite values that should be interpreted with suitable caution, especially the k_2 value when very large nanoparticles are involved.

A final take-home message, one fortified by the discussion in the SI, is that there can be little doubt that much remains to be learned about the intervening, underlying, $>10^7$ elementary steps that one deduces must be involved in the formation of large, $Ag(0)_n$ or other, ∼100 nm nanoparticles. Only the first-pass, initial start at kinetically and mechanistically characterizing these intriguing reactions has been achieved by the superb HEXRD data gathered in 2016[1] and its analysis in just two pseudoelementary steps and two associated, averaged rate constants—itself a remarkable result.

■ ASSOCIATED CONTENT

Supporting Information

The Supporting Information is available free of charge on the ACS Publications website at DOI: 10.1021/acs.jpcc.7b06323.

Derivation of kinetics equations employed for curve fitting and associated Figures S1, S2, S3, and S4, and discussion of Figure S2 about the probable composite nature of the observed two-step (apparent) rate constants; section S2: fitting the kinetics data to the bimolecular nucleation plus autocatalytic agglomeration

DOI: 10.1021/acs.jpcc.7b06323
J. Phys. Chem. C 2017, 121, 27643−27654

mechanism and associated Figure S5; section S3; estimation of the fraction of surface atoms in a 100 nm $Ag(0)_n$ nanoparticle; and section S4: further discussion of five questions and issues that have arisen in this research, and associated Figures S6 and S7 (PDF)

AUTHOR INFORMATION

Corresponding Author

*E-mail: Richard.Finke@colostate.edu.

ORCID

Saim Özkar: 0000-0002-6302-1429

Richard G. Finke: 0000-0002-3668-7903

Present Address

§(S.O.): Department of Chemistry, Colorado State University, Fort Collins, Colorado 80523, United States

Notes

The authors declare no competing financial interest.

ACKNOWLEDGMENTS

We thank Dr. Y. Sun for reading the penultimate version of this paper and for sharing his comments, questions, and concerns, a number of which we have striven to address in the main text and in the SI. His open sharing and intellectual independence are noteworthy and have contributed in a major way to the present work. This work was supported at Colorado State University by the U.S. Department of Energy (DOE), Office of Science, Office of Basic Energy Sciences, Division of Chemical Sciences, Geosciences & Biosciences, by DOE Grant SE-FG402-03ER15453.

REFERENCES

(1) Liu, Q.; Gao, M. R.; Liu, Y.; Okasinski, J. S.; Ren, Y.; Sun, Y. Quantifying the Nucleation and Growth Kinetics of Microwave Nanochemistry Enabled by in Situ High-Energy X-Ray Scattering. *Nano Lett.* **2016**, *16*, 715−720.

(2) Nishioka, M.; Miyakawa, M.; Kataoka, H.; Koda, H.; Sato, K.; Suzuki, T. M. Continuous Synthesis of Monodispersed Silver Nanoparticles Using a Homogeneous Heating Microwave Reactor System. *Nanoscale* **2011**, *3*, 2621−2626.

(3) Ott, L. S.; Finke, R. G. Transition-Metal Nanocluster Stabilization versus Agglomeration Fundamental Studies: Measurement of the Two Types of Rate Constants for Agglomeration Plus Their Activation Parameters under Catalytic Conditions. *Chem. Mater.* **2008**, *20*, 2592−2601.

(4) Finney, E. E.; Finke, R. G. The Four-Step, Double-Autocatalytic Mechanism for Transition-Metal Nanocluster Nucleation, Growth, and Then Agglomeration: Metal, Ligand, Concentration, Temperature, and Solvent Dependency Studies. *Chem. Mater.* **2008**, *20*, 1956−1970.

(5) Watzky, M. A.; Finney, E. E.; Finke, R. G. Transition-Metal Nanocluster Size vs Formation Time and the Catalytically Effective Nucleus Number: A Mechanism-Based Treatment. *J. Am. Chem. Soc.* **2008**, *130*, 11959−11969.

(6) Finney, E. E.; Finke, R. G. Fitting and Interpreting Transition-Metal Nanocluster Formation and Other Sigmoidal-Appearing Kinetic Data: A More Thorough Testing of Dispersive Kinetic vs Chemical-Mechanism-Based Equations and Treatments for 4-Step Type Kinetic Data. *Chem. Mater.* **2009**, *21*, 4468−4479.

(7) Finney, E. E.; Finke, R. G. Fitting and Interpreting Transition-Metal Nanocluster Formation and Other Sigmoidal-Appearing Kinetic Data: A More Thorough Testing of Dispersive Kinetic vs Chemical-Mechanism-Based Equations and Treatments for 4-Step Type Kinetic Data. *Chem. Mater.* **2010**, *22*, 2687−2688.

(8) Kytsya, A.; Bazylyak, L.; Hrynda, Y.; Horechyy, A.; Medvedevdkikh, Y. The Kinetic Rate Law for the Autocatalytic Growth of Citrate-Stabilized Silver Nanoparticles. *Int. J. Chem. Kinet.* **2015**, *47*, 351−360.

(9) Stamplecoskie, K. G.; Scaiano, J. C. Kinetics of the Formation of Silver Dimers: Early Stages in the Formation of Silver Nanoparticles. *J. Am. Chem. Soc.* **2011**, *133*, 3913−3920.

(10) Helmlinger, J.; Heise, M.; Heggen, M.; Ruck, M.; Epple, M. A Rapid, High-Yield and Large-Scale Synthesis of Uniform Spherical Silver Nanoparticles by a Microwave-Assisted Polyol Process. *RSC Adv.* **2015**, *5*, 92144−92150.

(11) Wang, Y.; Zheng, Y.; Huang, C. Z.; Xia, Y. Synthesis of Ag Nanocubes 18−32 nm in Edge Length: The Effects of Polyol on Reduction Kinetics, Size Control, and Reproducibility. *J. Am. Chem. Soc.* **2013**, *135*, 1941−1951.

(12) Besson, C.; Finney, E. E.; Finke, R. G. A Mechanism for Transition-Metal Nanoparticle Self-Assembly. *J. Am. Chem. Soc.* **2005**, *127*, 8179−8184.

(13) Özkar, S.; Finke, R. G. Nanoparticle Nucleation Is Termolecular in Metal and Involves Hydrogen: Evidence for a Kinetically Effective Nucleus of Three $\{Ir_3H_{2x}{\cdot}P_2W_{15}Nb_3O_{62}\}^{6-}$ in $Ir(0)_n$ Nanoparticle Formation From $[(1,5\text{-COD})Ir^{I}{\cdot}P_2W_{15}Nb_3O_{62}]^{8-}$ Plus Dihydrogen. *J. Am. Chem. Soc.* **2017**, *139*, 5444−5457.

(14) Laxson, W. W.; Finke, R. G. Nucleation is Second Order: An Apparent Kinetically Effective Nucleus of Two for Ir(0)*n* Nanoparticle Formation from $[(1,5\text{-COD})Ir^{I}{\cdot}P_2W_{15}Nb_3O_{62}]^{8-}$ Plus Hydrogen. *J. Am. Chem. Soc.* **2014**, *136*, 17601−17615.

(15) Watzky, M. A.; Finke, R. G. Transition Metal Nanocluster Formation Kinetic and Mechanistic Studies. A New Mechanism When Hydrogen Is the Reductant: Slow, Continuous Nucleation and Fast Autocatalytic Surface Growth. *J. Am. Chem. Soc.* **1997**, *119*, 10382−10400.

(16) Esepnson, J. H. *Chemical Kinetics and Reaction Mechanisms*, 2nd ed.; McGraw-Hill, Inc.: New York, 1995.

(17) Watzky, M. A.; Finke, R. G. Nanocluster Size-Control and "Magic Number" Investigations. Experimental Tests of the "Living-Metal Polymer" Concept and of Mechanism-Based Size-Control Predictions Leading to the Syntheses of Iridium(0) Nanoclusters Centering about Four Sequential Magic Numbers. *Chem. Mater.* **1997**, *9*, 3083−3095.

(18) Widegren, J. A.; Aiken, J. D., III; Özkar, S.; Finke, R. G. Additional Investigations of a New Kinetic Method To Follow Transition-Metal Nanocluster Formation, Including the Discovery of Heterolytic Hydrogen Activation in Nanocluster Nucleation Reactions. *Chem. Mater.* **2001**, *13*, 312−324.

(19) Wertz, D. L. Mass Absorption Corrected X-Ray Powder Diffractograms. Part 1: Measuring Pyrite in Powdered Coals. *Powder Diffr.* **1990**, *5*, 44−47.

(20) El Osta, R.; Feyand, M.; Stock, N.; Millange, F.; Walton, R. I. Crystallisation Kinetics of Metal Organic Frameworks From in situ Time-Resolved X-ray Diffraction. *Powder Diffr.* **2013**, *28*, S256−S275.

(21) Roselle, P. Quantitative Mineralogical Analysis of Carbonate Sediments by X-ray Diffraction: A New, Automatic Method for Sediments with Low Carbonate Content. *Sedimentology* **1982**, *29*, 595−600.

(22) Finney, E. E.; Finke, R. G. Is There a Minimal Chemical Mechanism Underlying Classical Avrami-Erofe'ev Treatments of Phase-Transformation Kinetic Data? *Chem. Mater.* **2009**, *21*, 4692−4705.

(23) Bentea, L.; Watzky, M. A.; Finke, R. G. Sigmoidal Nucleation and Growth Curves Across Nature Fit by the Finke−Watzky Model of Slow Continuous Nucleation and Autocatalytic Growth: Explicit Formulas for the Lag and Growth Times Plus Other Key Insights. *J. Phys. Chem. C* **2017**, *121*, 5302−5312.

(24) Widegren, J. A.; Bennett, M. A.; Finke, R. G. Is It Homogeneous or Heterogeneous Catalysis? Identification of Bulk Ruthenium Metal as the True Catalyst in Benzene Hydrogenations Starting with the Monometallic Precursor, $Ru(II)(\eta^6\text{-}C_6Me_6)(OAc)_2$, Plus Kinetic

DOI: 10.1021/acs.jpcc.7b06323
J. Phys. Chem. C 2017, 121, 27643−27654

Characterization of the Heterogeneous Nucleation, then Autocatalytic Surface-Growth Mechanism. *J. Am. Chem. Soc.* **2003**, *125*, 10301.
(25) Lin, Y.; Finke, R. G. A More General Approach to Distinguishing 'Homogeneous' from 'Heterogeneous' Catalysis: Discovery of Polyoxoanion and Bu_4N^+ -Stabilized, Isolable and Redissolvable, High Reactivity $Ir_{\sim 190-450}$ Nanocluster Catalysts. *Inorg. Chem.* **1994**, *33*, 4891.
(26) Starkey Ott, L.; Finke, R. G. Supersensitivity of Ir(0)n Transition-Metal Nanoparticle Formation to Initial Ir Precursor Concentration and Reaction Temperature. Understanding Its Origins. *J. Nanosci. Nanotechnol.* **2008**, *8*, 1551−1556.
(27) Seshadri, I.; Esquenazi, G. L.; Cardinal, T.; Borca-Tasciuc, T.; Ramanath, G. Microwave Synthesis of Branched Silver Nanowires and Their Use as Fillers for High Thermal Conductivity Polymer Composites. *Nanotechnology* **2016**, *27*, 175601.
(28) Xiong, Y.; Siekkinen, A. R.; Wang, J.; Yin, Y.; Kim, M. J.; Xia, Y. Synthesis of Silver Nanoplates at High Yields by Slowing Down the Polyol Reduction of Silver Nitrate with Polyacrylamide. *J. Mater. Chem.* **2007**, *17*, 2600−2602.
(29) Tang, Y.; He, W.; Zhou, G.; Wang, S.; Yang, X.; Tao, Z.; Zhou, J. Z. A New Approach Causing the Patterns Fabricated by Silver Nanoparticles to be Conductive Without Sintering. *Nanotechnology* **2012**, *23*, 355304.
(30) Kang, M. G.; Guo, L. J. Nanoimprinted Semitransparent Metal Electrodes and Their Application in Organic Light-Emitting diodes. *Adv. Mater.* **2007**, *19*, 1391−1396.
(31) Starkey Ott, L.; Finke, R. G. Transition-metal Nanocluster Stabilization for Catalysis: A Critical Review of Ranking Methods and Putative Stabilizers. *Coord. Chem. Rev.* **2007**, *251*, 1075−1100.
(32) Lin, Y.; Finke, R. G. Novel Polyoxoanion- and Bu_4N^+-Stabilized, Isolable, and Redissolvable, 20−30 Å $Ir_{300-900}$ Nanoclusters: The Kinetically Controlled Synthesis, Characterization, and Mechanism of Formation of Organic Solvent-Soluble, Reproducible Size, and Reproducible Catalytic Activity Metal Nanoclusters. *J. Am. Chem. Soc.* **1994**, *116*, 8335−8353.
(33) Özkar, S.; Finke, R. G. Nanocluster Formation and Stabilization Fundamental Studies: Ranking Commonly Employed Anionic Stabilizers via the Development, Then Application, of Five Comparative Criteria. *J. Am. Chem. Soc.* **2002**, *124*, 5796−5810.
(34) Aiken, J. D., III; Finke, R. G. Nanocluster Formation Synthetic, Kinetic, and Mechanistic Studies. The Detection of, and Then Methods To Avoid, Hydrogen Mass-Transfer Limitations in the Synthesis of Polyoxoanion- and Tetrabutylammonium-Stabilized, Near-Monodisperse 40 ± 6 Å Rh(0) Nanoclusters. *J. Am. Chem. Soc.* **1998**, *120*, 9545−9554.
(35) Wiley, B.; Sun, Y.; Xia, Y. Polyol Synthesis of Silver Nanostructures: Control of Product Morphology with Fe(II) or Fe(III) Species. *Langmuir* **2005**, *21*, 8077−8080.
(36) Nakano, M.; Fujiwara, T.; Koga, N. Thermal Decomposition of Silver Acetate: Physico-Geometrical Kinetic Features and Formation of Silver Nanoparticles. *J. Phys. Chem. C* **2016**, *120*, 8841−8854.
(37) Harada, M.; Kizaki, S. Formation Mechanism of Gold Nanoparticles Synthesized by Photoreduction in Aqueous Ethanol Solutions of Polymers Using In Situ Quick Scanning X-ray Absorption Fine Structure and Small-Angle X-ray Scattering. *Cryst. Growth Des.* **2016**, *16*, 1200−1212.
(38) Tatarchuk, V. V.; Sergievskaya, A. P.; Korda, T. M.; Druzhinina, I. A.; Zaikovsky, V. I. Kinetic Factors in the Synthesis of Silver Nanoparticles by Reduction of Ag^+ with Hydrazine in Reverse Micelles of Triton N-42. *Chem. Mater.* **2013**, *25*, 3570−3579.
(39) Smith, S. E.; Sasaki, J. M.; Bergman, R. G.; Mondloch, J. E.; Finke, R. G. Platinum-Catalyzed Phenyl and Methyl Group Transfer from Tin to Iridium: Evidence for an Autocatalytic Reaction Pathway with an Unusual Preference for Methyl Transfer. *J. Am. Chem. Soc.* **2008**, *130*, 1839−1841.
(40) Tong, F.; Hanson, M. P.; Bardeen, C. J. Analysis of Reaction Kinetics in the Photomechanical Molecular Crystal 9-Methylanthracene Using and Extended Finke-Watzky Model. *Phys. Chem. Chem. Phys.* **2016**, *18*, 31936−31945.
(41) Platt, J. R. Strong Inference. *Science* **1964**, *146*, 347.
(42) Frost, A. A.; Pearson, R. G. *Kinetics and Mechanism, A Study of Homogeneous Chemical Reactions*, 2nd ed.; John Wiley & Sons: New York, 1961.
(43) Ashley, B.; Vakil, P. N.; Lynch, B. B.; Dyer, C. M.; Tracy, J. B.; Owens, J.; Strouse, G. F. Microwave Enhancement of Autocatalytic Growth of Nanometals. *ACS Nano* **2017**, *11*, 9957−9967.

NOTE ADDED IN PROOF

A paper by G. F. Strouse and co-workers has appeared[43] that supports the findings of present studies. Specifically, that 2017 paper studies primarily Ni, but also Au, nanoparticle (NP) formatting under microwave (MW) heating, and includes in its conclusions the following: (i) "It is demonstrated that the MW facilitated growth of metal NPs follows the FW autocatalytic model"; and (ii) "The power-dependent enhancement in the dispersity for NPs grown in an MW is readily explained within the FW autocatalytic mechanism without involving MW special effects".

DOI: 10.1021/acs.jpcc.7b06323
J. Phys. Chem. C 2017, 121, 27643−27654